2014년 12월 전자공학회 논문지 제 51권 제 12 호
Journal of The Institute of Electronics and Information Engineers Vol. 51, NO. 12, December 2014 http://dx.doi.org/10.5573/ieie.2014.51.12.059

논문 2014-51-12-6

Sub-micron MOSFET을 위한 입력 저항의 게이트 핑거 수 종속성 측정 및 분석

(Measurement and Analysis of Gate Finger Number Dependence of Input Resistance for Sub-micron MOSFETs)

안 자 현*, 이 성 현**

(Jahyun Ahn and Seonghearn Lee©)

요 약

다양한 게이트 핑거 수(Nf)의 MOSFET에 대한 두 종류의 입력 저항이 S_{11}-parameter와 Z_{11}-parameter으로부터 변환되어 저주파 영역에서 측정되었다. 본 연구에서 사용된 Nf ≤ 64의 범위에서 S_{11}-parameter로부터 추출된 1/Nf 종속 입력저항은 Z_{11}-parameter로부터 추출된 입력 저항보다 훨씬 낮은 값을 보여주며, 이러한 1/Nf 종속성은 MOSFET의 등가회로로부터 유도된 Nf 종속 비선형 방정식으로부터 이론적으로 증명하였다.

Abstract

Two input resistances converted from S_{11}-parameter and Z_{11}-parameter of MOSFETs with various gate finger numbers Nf were measured in low frequency region. The 1/Nf dependent input resistance from S_{11}-parameter exhibits much lower values than that from Z_{11}-parameter in the range of Nf ≤ 64. This 1/Nf dependence was theoretically verified by using Nf dependent nonlinear equation derived from a MOSFET equivalent circuit.

Keywords: MOSFET, input resistance, S-parameter, Z-parameter, gate finger number

I. Introduction

Recently, as the gate length L_g of a MOSFET is gradually reduced with the development of process technology, the MOSFET with a high process stability, a high integration, and excellent price competitiveness is widely used as a basic device to fabricate RF ICs. The maximum oscillation frequency fmax and noise figure are improved because the gate resistance R_g is reduced by a multi-finger gate layout[1].

The prediction of input resistance R_{IN} scalability according to the number of gate finger Nf variation is very important to design the input impedance matching block of a RF integrated circuit (IC) with multi-finger MOSFETs. It is generally known that R_{IN} is affected by only R_g. However, this is no longer valid in accordance with the reduction of L_g of short-channel devices in the saturation region. As L_g is scaled down to deep sub-micron, R_{IN} is increased

* 학생회원, ** 정회원, 한국외국어대학교 전자공학과
(Department of Electronics Engineering, Hankuk University of Foreign Studies)
© Corresponding Author(E-mail: shlee@hufs.ac.kr)
※ 이 연구는 2014학년도 한국외국어대학교 교내학술연구비의 지원에 의하여 이루어진 것임.
접수일자: 2014년09월24일, 수정일자: 2014년11월24일
게재확정: 2014년12월02일

even in the low frequency range by another component due to the output resistance connected to the drain in the saturation region[2~3]. The low-frequency R_{IN} is still important in RF IC design, because it strongly affects the high-frequency response of R_{IN} up to the 3-dB cutoff frequency.

Thus, R_{IN} converted from S_{11}-parameter with the load resistance of 50Ω connected in output port is different from R_{IN} from Z_{11}-parameter with opened output port. Since S-parameter data are widely used in RF IC design, it is important to study the characteristics of Nf dependent scalability of R_{IN} for S-parameter measurement network. However, a study on the Nf dependence has not been carried out in previous papers[2~3] related to R_{IN}.

Therefore in this paper, Nf dependent equation of low-frequency R_{IN} measured from S_{11}-parameter of multi-finger sub-micron MOSFETs is derived and scalability characteristics are analyzed in detail.

II. Measurement and Analysis

1. Input Resistance Measurement

N-MOSFETs with multi-finger gate (L_g = 0.18 μm, the unit gate finger width Wu = 10㎛ , Nf= 4 – 64) were used in this work. S-parameters of these devices were measured by a vector network analyzer using on-wafer RF probe installed in a wafer probe station.

We carried out a de-embedding process for removing RF probe pad and metal interconnection parasitic components from measured S-parameters using an open test pattern with opened device area and short test pattern with shorted device area[4].

According to a circuit theory, the input impedance is changed in accordance with two-port measurement system. Therefore, two different input resistances are defined by the following formulas[5].

$$R_{IN(S)} = Z_o \cdot Real\left[\frac{1+S_{11}}{1-S_{11}}\right] \quad (1)$$

$$R_{IN(Z)} = Real\left[Z_{11}\right] \quad (2)$$

where $R_{IN(S)}$ is the input resistance converted from S_{11}-parameter, $R_{IN(Z)}$ is the input resistance converted from Z_{11}-parameter, and Z_O is the characteristic impedance of R_O =50Ω.

Fig. 1 shows the frequency response of (1) and (2). Due to the series gate capacitances, $R_{IN(S)}$ and $R_{IN(Z)}$ decrease with frequency. To remove the capacitance effect, $R_{IN(S)LF}$ and $R_{IN(Z)LF}$ obtained from low -frequency (LF) data of (1) and (2) respectively are used to analyze the general characteristics of 1/Nf dependency. In this work, the lowest frequency range of about 0.7 GHz without any abnormal fluctuation is used to determine the input resistance.

Fig. 2 shows $R_{IN(S)LF}$ and $R_{IN(Z)LF}$ as a function of

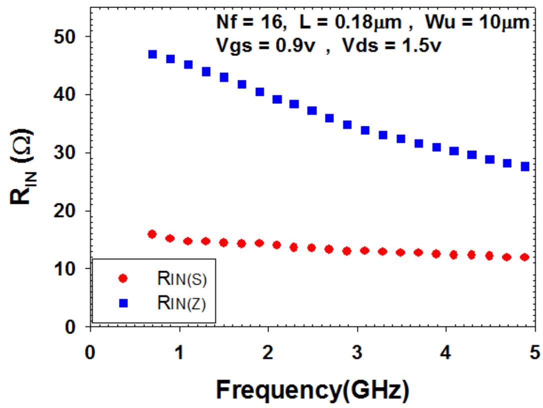

그림 1. $R_{IN(S)}$와 $R_{IN(Z)}$의 주파수 응답.
Fig. 1. Frequency response of $R_{IN(S)}$ and $R_{IN(Z)}$.

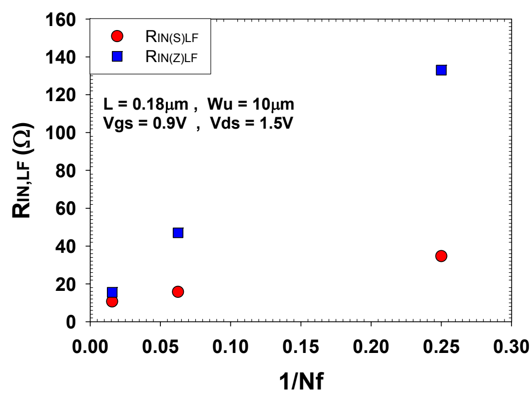

그림 2. $R_{IN(S)LF}$와 $R_{IN(Z)LF}$ 대 1/Nf 그래프.
Fig. 2. $R_{IN(S)LF}$ and $R_{IN(Z)LF}$ versus 1/Nf graph.

1/Nf. The values of $R_{IN(S)LF}$ are much lower than that of $R_{IN(Z)LF}$. This difference is generated by different measurement systems for two-port parameters.

However, these Nf dependent characteristics of R_{IN} have not been reported yet. Therefore, the physical origin and analysis for Nf dependent R_{IN} depending on two-port measurement parameters are performed in the next chapter.

1. Input Resistance Equation

In order to theoretically analyze the cause of Nf dependence difference of R_{IN}, $R_{IN(S)LF}$ and $R_{IN(Z)LF}$ were derived using a MOSFET small-signal equivalent circuit of Fig. 3[6~8].

In S_{11}-parameter measurement system, the circuit equation of $R_{IN(S)LF}$ is derived in low frequency region using a simplified input equivalent circuit of Fig. 4 where the load resistance of Z_o = R_o = 50Ω is connected in output port. The substrate block(C_{jd}, C_{bk},

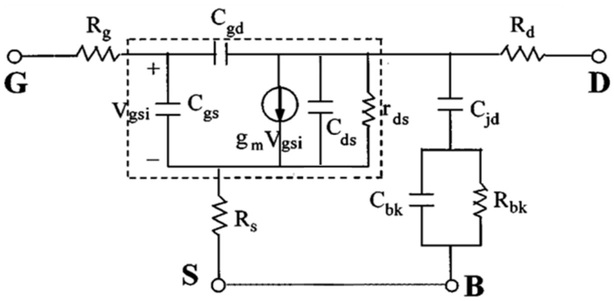

그림 3. MOSFET 소신호 등가회로.
Fig. 3. Small-signal MOSFET equivalent circuit.

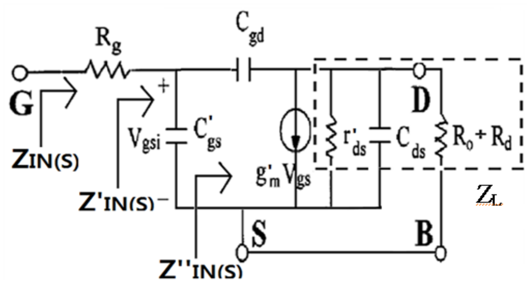

그림 4. S_{11}-parameter 측정시스템의 저주파영역에서 기판 블록이 무시된 단순화된 입력 등가회로.
Fig. 4. The simplified input equivalent circuit with neglecting a substrate block at low frequencies in the S_{11}-parameter measurement system.

R_{bk}) is ignored in low frequency region. In Fig. 4, the negative feedback resistance R_s is absorbed in the formulas of C'_{gs}, g'_m and r'_{ds} by combining with C_{gs}, g_m and r_{ds}[3, 9].

$$C'_{gs} = \frac{C_{gs}}{1+g_m R_s} \tag{3}$$

$$r'_{ds} = r_{ds}(1+g_m R_s) \tag{4}$$

$$g'_m = \frac{g_m}{1+g_m R_s} \tag{5}$$

$$C'_{ds} = \frac{C_{ds}}{1+g_m R_s} \tag{6}$$

In Fig. 4, $Z'_{IN(S)}$ is the input impedance seen in front of C'_{gs} and $Z''_{IN(S)}$ is one behind C'_{gs}. The effective load impedance Z_L in a dashed box is a parallel block with r'_{ds}, C'_{ds} and R_o + R_d. From Fig. 4, $Z''_{IN(S)}$ is derived by the following equation.

$$Z''_{IN(S)} = \frac{\frac{1}{jwC_{gd}} + Z_L}{g'_m Z_L + 1} \tag{7}$$

From Fig. 4, $R'_{IN(S)}$ is expressed by the real part of the parallel impedance of $Z''_{IN(S)}$ and C'_{gs}.

$$R'_{IN(S)} = Real\left[\frac{\frac{1}{jwC'_{gs}} Z''_{IN(S)}}{\frac{1}{jwC'_{gs}} + Z''_{IN(S)}}\right] \tag{8}$$

Substituting (7) into (8), the following equation is derived:

$$R'_{IN(S)} = \frac{R_L\left\{1+g'_m R_L\left(1+\frac{C'_{ds}}{C_{gd}}\right)\right\}}{w^2 R_L^2 (C'_{gs}C'_{ds} + C_{gd}C'_{ds} + C'_{gs}C_{gd})^2 + \left(\frac{C'_{gs}}{C_{gd}} + g'_m R_L + 1\right)^2} \tag{9}$$

where R_L is parallel resistance of r'_{ds} and R_o+R_d in Fig. 4.

In the low-frequency (LF) region where ω << $[(C'_{gs}/C_{gd})+g'_m R_L+1]/R_L(C'_{gs}C'_{ds}+C_{gd}C'_{ds}+C'_{gs}C_{gd})$, (9) can be approximated by the following formula:

$$R'_{IN(S)LF} \approx \frac{R_L\left\{1+g'_m R_L\left(1+\frac{C'_{ds}}{C_{gd}}\right)\right\}}{\left(\frac{C'_{gs}}{C_{gd}}+g'_m R_L+1\right)^2} \tag{10}$$

In Z-parameter measurement system, R_o is replaced by infinite resistance due to opened drain output port in Fig. 4. Since R_L = r'_{ds}, $R'_{IN(Z)LF}$ in (10) is changed into:

$$R'_{IN(Z)LF} \approx \frac{r'_{ds}\left\{1+g'_m r'_{ds}\left(1+\frac{C'_{ds}}{C_{gd}}\right)\right\}}{\left(\frac{C'_{gs}}{C_{gd}}+g'_m r'_{ds}+1\right)^2} \tag{11}$$

3. Extraction of Nf Scalable Parameters

In order to analyze Nf dependence of derived $R'_{IN(S)LF}$ and $R'_{IN(Z)LF}$ of (10) and (11), Nf dependent equations for MOSFET equivalent circuit parameters of Fig. 3 are extracted as follows:

In high-frequency region where frequency dependency disappears, gate resistance R_g, the drain resistance R_d, and source resistance R_s are extracted at $V_{ds}=V_{gs}=0V$ by y-intercepts of (12), (13) and (14) versus ω^{-2}, respectively[6~7]:

$$Real[Z_{11}-Z_{12}] \approx R_g + A_g\omega^{-2} \tag{12}$$

$$Real[Z_{22}-Z_{12}] \approx R_d + A_d\omega^{-2} \tag{13}$$

$$Real[Z_{12}] \approx R_s + A_s\omega^{-2} \tag{14}$$

Junction and substrate parameters (C_{jd}, R_{bk}, C_{bk}) are extracted by a direct extraction method[7,8] using Y^d-parameters without R_d at $V_{gs}=0V$, $V_{ds}=1.5V$. After intrinsic Y^i-parameters are obtained by removing C_{jd}, R_{bk}, C_{bk}, R_g and R_s from the Y^d-parameters at $V_{gs}=0.9V$, $V_{ds}=1.5V$, the drain-source resistance r_{ds} and transconductance g_m are extracted by[6,7]:

$$r_{ds} = \frac{1}{Real[Y^i_{22}]} \tag{15}$$

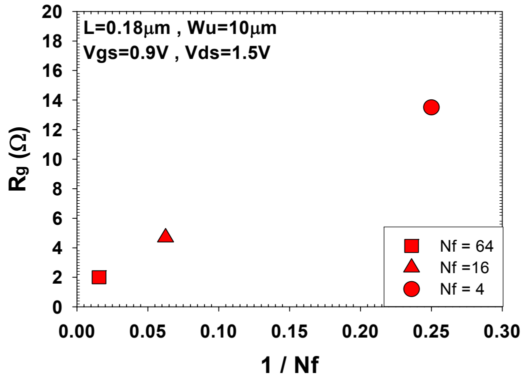

그림 5. 식(12)로 추출된 R_g 대 1/Nf 그래프
Fig. 5. Extracted R_g using (12) versus 1/Nf graph.

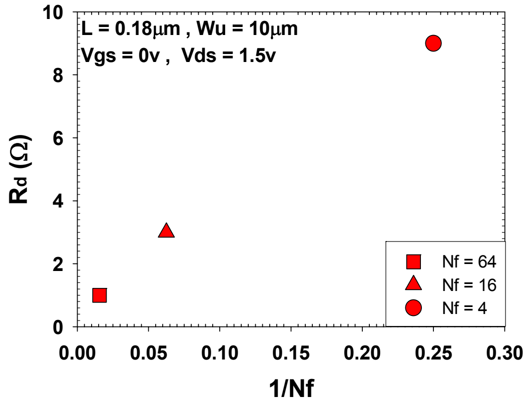

그림 6. 식(13)으로 추출된 R_d 대 1/Nf 그래프.
Fig. 6. Extracted R_d using (13) versus 1/Nf graph.

$$g_m = |Y^i_{21} - Y^i_{12}| \tag{16}$$

The Nf dependent values of r'_{ds} and g'_m are obtained by substituting extracted R_s, r_{ds} and g_m into (4) and (5), respectively. In Figs. 5-7, R_g, R_d and r'_{ds} are plotted as a function of 1/Nf, respectively. Fig. 8 shows the extracted g'_m as a function of Nf.

As shown in Figs. 5-8, R_g, R_d and r'_{ds} are linearly scaled by 1/Nf and g'_m is by Nf.

Thus, these MOSFET parameters can be expressed by following scalable Nf dependent equations:

$$R_g = \frac{R_{gu}}{Nf} \tag{17}$$

$$R_d = \frac{R_{du}}{Nf} \tag{18}$$

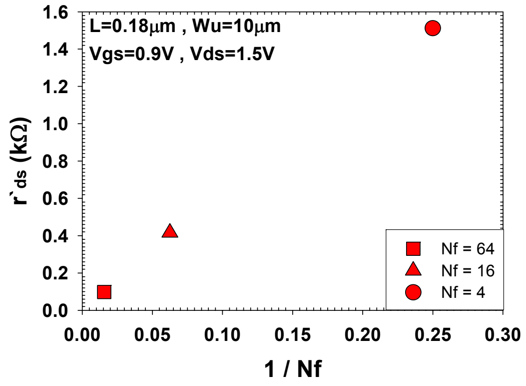

그림 7. 추출된 r'_{ds} 대 1/Nf 그래프.
Fig. 7. Extracted r'_{ds} versus 1/Nf graph.

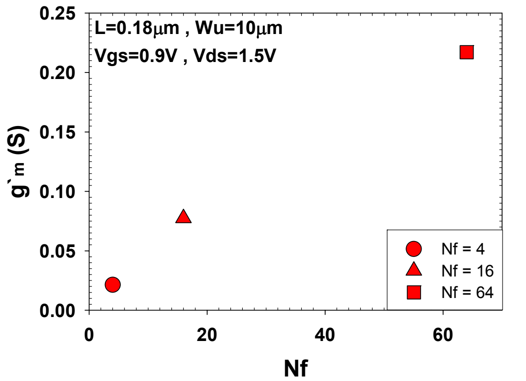

그림 8. 추출된 g'_m 대 Nf 그래프.
Fig. 8. Extracted g'_m versus Nf graph.

$$r'_{ds} = \frac{r'_{dsu}}{Nf} \tag{19}$$

$$g'_m = g'_{mu} Nf \tag{20}$$

where R_{gu}, R_{du}, g'_{mu} and r'_{dsu} are the values at the unit finger and extracted from slopes of Figs. 5-8, respectively. The Nf-dependent equations of (17)-(20) is physically acceptable because unit finger devices are connected in parallel for a multi-finger layout.

4. Analysis of 1/Nf Dependence

In order to obtain 1/Nf dependence of only $R'_{IN(S)LF}$ and $R'_{IN(Z)LF}$ in Fig. 4, the extracted R_g in Fig. 5 is removed from $R_{IN(S)LF}$ and $R_{IN(Z)LF}$ of Fig. 2. In Fig 9, $R'_{IN(S)LF}$ has much lower values than $R'_{IN(Z)LF}$.

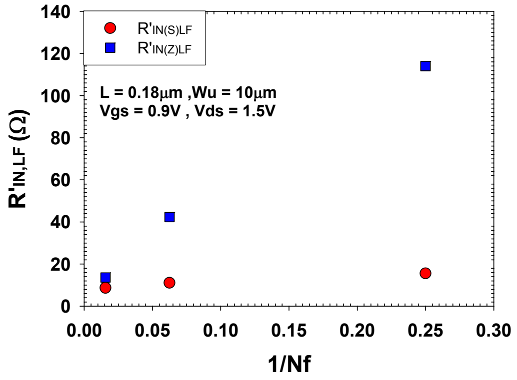

그림 9. $R'_{IN(S)LF}$와 $R'_{IN(Z)LF}$ 대 1/Nf 그래프.
Fig. 9. $R'_{IN(S)LF}$ and $R'_{IN(Z)LF}$ versus 1/Nf graph.

In order to analyze this scalability characteristics of the input resistance, Nf dependent equations for (10) and (11) are derived as follows:

By substituting (19) and (20) into (11), $R'_{IN(Z)LF}$ is expressed by the following Nf dependent equation:

$$R'_{IN(Z)LF} \approx \frac{\frac{r'_{dsu}}{Nf}\left\{1 + g'_{mu} r'_{dsu}\left(1 + \frac{C_{ds}}{C_{gd}}\right)\right\}}{\left(\frac{C'_{gs}}{C_{gd}} + g'_{mu} r'_{dsu} + 1\right)^2} \tag{21}$$

In (21), C'_{ds}/C_{gd} and C'_{gs}/C_{gd} are unrelated with Nf because C'_{ds}, C_{gd} and C'_{gs} are proportional to Nf. Thus, $R'_{IN(Z)LF}$ shows the simple linear dependence of 1/Nf and good agreement with Fig 9. If extracted model parameters are used for (21), $R'_{IN(Z)LF}$ is calculated to be large values like Fig. 9.

However, the Nf dependent equation for $R'_{IN(S)LF}$ is more complex than that of $R'_{IN(Z)LF}$, because R_L in Fig. 4 is expressed as follows:

$$R_L = \frac{r'_{ds}(R_o + R_d)}{r'_{ds} + (R_o + R_d)} \tag{22}$$

By substituting (18) and (19), (22) is rewritten by the following equation:.

$$R_L = \frac{r'_{dsu}(NfR_o + R_{du})}{Nf(r'_{dsu} + NfR_o + R_{du})} \tag{23}$$

Since R_{du}(=36Ω) << r'_{dsu}(= 6,186Ω) from the slope of Figs. 6 and 7, (23) is approximated by:

$$R_L \approx \frac{r'_{dsu}(NfR_o + R_{du})}{Nf(r'_{dsu} + NfR_o)} \tag{24}$$

If Nf_o is defined by a value of Nf at a half R_L, it is equal to r'_{dsu} / R_o. It is determined that Nf_o = r'_{dsu} / R_o = 120. Thus, (24) is rewritten by the following Nf nonlinear equation:

$$R_L \approx \frac{R_0 + \dfrac{R_{du}}{Nf}}{1 + \dfrac{Nf}{Nf_0}} \tag{25}$$

Due to R_L in (25), $R'_{IN(S)LF}$ in (10) exhibits the nonlinear Nf dependent characteristics.

If Nf >> Nf_o in (25), R_{du}/Nf << R_o. Thus, R_L is simplified by r'_{ds} of (19):

$$R_L \approx \frac{r'_{dsu}}{Nf} \tag{26}$$

Substituting (26) into (10) gives the following equation of $R'_{IN(S)LF}$ that is same as $R'_{IN(Z)LF}$ of (21):

$$R'_{IN(S)LF} \approx \frac{\dfrac{r'_{dsu}}{Nf}\left\{1 + g'_{mu} r'_{dsu}\left(1 + \dfrac{C'_{ds}}{C_{gd}}\right)\right\}}{\left(\dfrac{C'_{gs}}{C_{gd}} + g'_{mu} r'_{dsu} + 1\right)^2} \tag{27}$$

If Nf << Nf_o, R_L of (25) is simplified by following equation.

$$R_L \approx R_0 + \frac{R_{du}}{Nf} \tag{28}$$

In this work, Nf << Nf_o because of Nf ≤ 64. Thus, by substituting (28) into (10), the Nf dependent equation of $R'_{IN(S)LF}$ can be derived as:

$$R'_{IN(S)LF} \approx \frac{(R_0 + \dfrac{R_{du}}{Nf})\left\{1 + g'_{mu}(R_0 Nf + R_{du})\left(1 + \dfrac{C_{ds}}{C_{gd}}\right)\right\}}{\left(\dfrac{C'_{gs}}{C_{gd}} + g'_{mu}(R_0 Nf + R_{du}) + 1\right)^2} \tag{29}$$

Substituting extracted model parameters in (29), $R'_{IN(S)LF}$ is calculated to be 12.5Ω at Nf=4, 13.3Ω at Nf=16, and 8.9Ω at Nf=64. Thus, as shown in Fig 9, the theoretical values of $R'_{IN(S)LF}$ are much lower than those of $R'_{IN(Z)LF}$. This weaker 1/Nf dependence of $R'_{IN(S)LF}$ than $R'_{IN(Z)LF}$ is originated from the R_o connected in output port for measuring S_{11}-parameter.

Especially, $R'_{IN(S)LF}$ increases with decreasing L_g because of the reduction of C'_{gs}/C_{gd} in saturation region due to the decrease of the channel capacitance under the constant overlap capacitance. Thus, as L_g is scaled down in deep sub-micron multi-finger MOSFETs, Nf dependent non-linear characteristics of (25) become more important in designing input matching circuit of RF IC.

Ⅲ. Conclusions

Two different kinds of input resistances in low-frequency region at various Nf devices were measured using S_{11}-parameter and Z_{11}-parameter. It is observed that a 1/Nf dependent plot of the input resistance converted from S_{11}-parameter has much lower values than that from Z_{11}-parameter in MOSFETs with Nf ≤ 64. This very weak 1/Nf dependence of input resistance converted from S_{11}-parameter was confirmed by Nf dependent nonlinear equation derived from a MOSFET equivalent circuit. It is revealed that this dependence is originated from the load resistance connected in output port for S_{11}-parameter measurements.

REFERENCES

[1] C. S. Kim, H. K. Yu, H. Cho, S. Lee, and K. S. Nam, “CMOS layout and bias optimization for RF IC design applications in IEEE MTT-S Int. Microwave Symp. Dig., pp. 945-948, 1997.

[2] Y.-S. Lin and S.-S. Lu, “An analysis small-signal gate-drain resistance effect on RF power MOSFETs,” IEEE Trans. Electron Devices, vol. 50, no. 2, February 2003.

[3] Y.-S. Lin, “An analysis of small-signal source-body resistance effect on RF MOSFETs for low-cost system-on-chip(SoC) applications,”

IEEE Trans. Electron Devices, vol. 52, no. 7, pp. 1442-1451, July 2005.

[4] J. Cha, J. Cha, and S. Lee, "Uncertainty analysis of two-step and three-step methods for deembedding on-wafer RF transistor measurements," IEEE Trans. Electron Device, Vol. 55, pp. 2195-2201, 2008.

[5] R. Ludwig and G. Bogdanov, RF Circuit Design Theory and Applications, 2nd Edition, Prentice Hall, pp. 182-183, 2010.

[6] S. Lee, C. S. Kim, and H. K. Yu, "A small-signal RF model and its parameter extraction for substrate effects in RF MOSFETs," IEEE Trans. Electron Devices, vol. 48, pp. 1374-1379, July 2001.

[7] J. Kim, Y. Lee, M. Choi, J. Koo, and S. Lee, "Gate-length dependent cutoff frequency extraction for nano-scale MOSFET," Journal of The Institute of Electronics Engineers of Korea - Semiconductor and Devices, vol. 42, no. 12, pp. 1-8, 2005.

[8] Y. Lee, M. Choi, J. Koo, and S. Lee, "Bias and gate-length dependent data extraction of substrate circuit parameters for deep submicron MOSFETs," Journal of The Institute of Electronics Engineers of Korea - Semiconductor and Devices, vol. 41, no. 12, pp. 27-34, 2004.

[9] S.-S. Lu, C. Meng, T.-W. Chen and H.-C. Chen, "The origin of the kink phenomenon of transistor scattering parameter S22," IEEE Transaction on Microwave Theory Techniques, vol. 49, no. 2, pp. 333-340, February 2001.

저 자 소 개

안 자 현(학생회원)
2014년 한국외국어대학교 전자공학과 학사 졸업.
2014년~현재 한국외국어대학교 전자정보공학과 석사과정.
<주관심분야 : RF CMOS 소자 모델링>

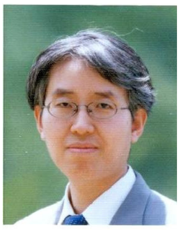

이 성 현(정회원)-교신저자
1985년 고려대학교 전자공학과 학사 졸업.
1989년 미국 University of Minnesota 전기공학과 석사 졸업.
1992년 미국 University of Minnesota 전기공학과 박사 졸업.
1992년~1995년 한국전자통신연구원 선임연구원
1995년~현재 한국외국어대학교 전자공학과 교수
<주관심분야 : CMOS 및 바이폴라 소자 모델링>